USGS
science for a changing world

Coastal Circulation and Sediment Dynamics along West Maui, Hawaii

PART III:

Flow and particulate dynamics during the 2003 summer coral spawning season

U.S. Department of the Interior
U.S. Geological Survey

Open-File Report 2004-1287

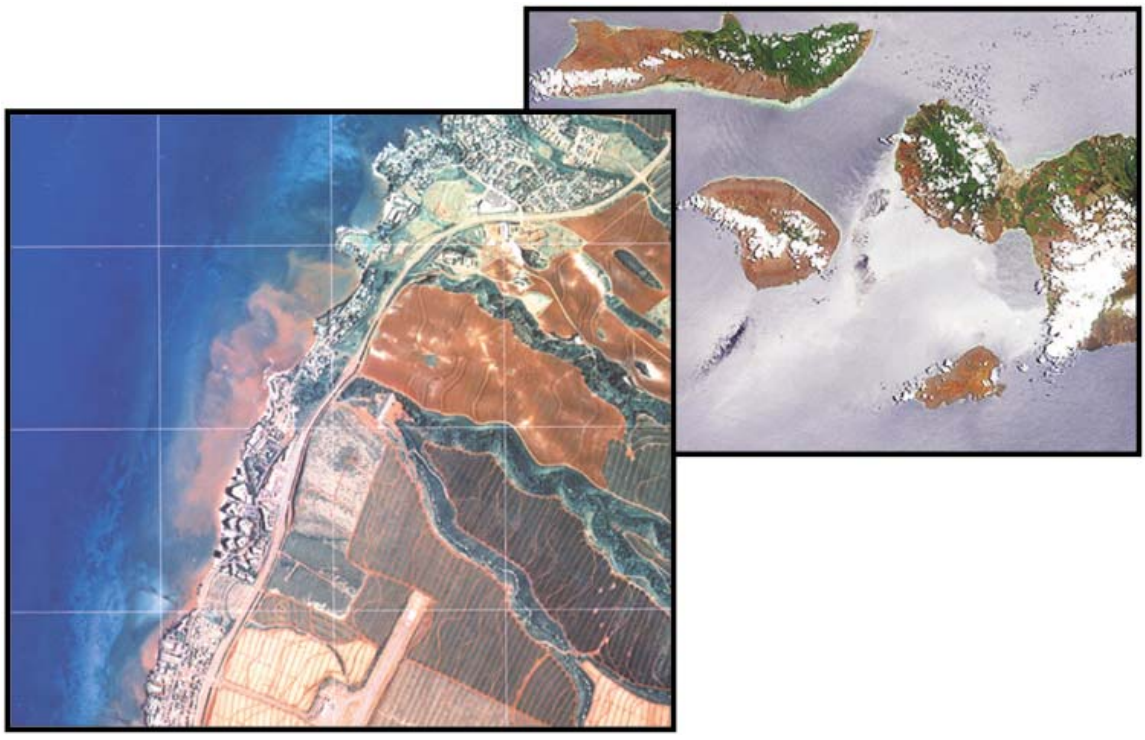

Coastal Circulation and Sediment Dynamics along West Maui, Hawaii

PART III:

Flow and particulate dynamics during the 2003 summer coral spawning season

Curt D. Storlazzi[1], Michael E. Field[1], Andrea S. Ogston[2], Joshua B. Logan[1], M. Kathy Presto[2] and Dave G. Gonzales[3]

[1]US Geological Survey, Pacific Science Center, Santa Cruz, CA
[2]University of Washington, School of Oceanography, Seattle, WA
[3]US Geological Survey, Western Region Marine Facility, Redwood City, CA

U.S. GEOLOGICAL SURVEY
Open-File Report 2004-1287

Santa Cruz, California
2004

LIST OF TABLES

LIST OF FIGURES

LIST OF APPENDICES

ADDITIONAL DIGITAL INFORMATION

For additional information on the instrument deployments, please see:
http://walrus.wr.usgs.gov/infobank/a/a201hw/html/a-4-03-hw.meta.html

For an online PDF version of this report, please see:
http://geopubs.wr.usgs.gov/open-file/of04-1287/

For more information on the U.S. Geological Survey Western Region's Coastal and Marine Geology Team, please see:
http://walrus.wr.usgs.gov/

For more information on the U.S. Geological Survey's Coral Reef Project, please see:
http://coralreefs.wr.usgs.gov/

DIRECT CONTACT INFORMATION

General Project Information
Dr. Michael E. Field (Project Chief): mfield@usgs.gov

Regarding this Report:
Dr. Curt D. Storlazzi (Lead Oceanographer): cstorlazzi@usgs.gov

REPORT REFERENCE

Storlazzi, C.D., Field, M.E., Ogston, A.S., Logan, J.B., Presto, M.K. and Gonzales, D.G., 2004. "Coastal Circulation and Sediment Dynamics along West Maui, Hawaii, PART III: Flow and particulate dynamics during the 2003 summer coral spawning season." *U.S. Geological Survey Open-File Report 2004-1287*, 36 p.

INTRODUCTION

High-resolution measurements of currents, temperature, salinity and turbidity were made over the course of three months off West Maui in the summer and early fall of 2003 to better understand coastal dynamics in coral reef habitats. Measurements were made through the emplacement of a series of bottom-mounted instruments in water depths less than 11 m. The studies were conducted in support of the U.S. Geological Survey (USGS) Coastal and Marine Geology Program's Coral Reef Project. The purpose of these measurements was to collect hydrographic data to better constrain the variability in currents and water column properties such as water temperature, salinity and turbidity in the vicinity of nearshore coral reef systems over the course of a summer and early fall when coral larvae spawn. These measurements support the ongoing process studies being conducted under the Coral Reef Project; the ultimate goal is to better understand the transport mechanisms of sediment, larvae, pollutants and other particles in coral reef settings. This report, the third in a series of three, describes data acquisition, processing and analysis. Previous reports provided data and results on: Long-term measurements of currents, temperature, salinity and turbidity off Kahana (PART I), and The spatial structure of currents, temperature, salinity and suspended sediment along West Maui (PART II).

Project Objectives:

The objective of these deployments was to understand how currents, temperature, salinity and turbidity vary temporally along West Maui over the course of the coral spawning season. These data were collected to support the ongoing process studies being conducted off northwest Maui as part of the USGS's multi-disciplinary Coral Reef Project that focuses on the geologic processes that affect coral reef systems. To meet these objectives, flow and water properties throughout the water column off West Maui were investigated. These data will provide information that can be used to understand pathways of terrestrial sediment, nutrient or contaminant delivery and coral larval transport on nearshore coral reefs. Instrument packages were deployed off West Maui over a period of three months spanning the mid summer and early fall seasons of 2003. Data collected during these deployments provided an intermediate spatial and temporal scale between the long-term baseline data collected between 2001 and early 2003 (see PART I of this report, Storlazzi and Jaffe, 2003) and the spatially-extensive but very short-term measurements made in the winter and summer of 2003 (see PART II of this report, Storlazzi et al., 2003).

Study Area:

These deployments were conducted offshore West Maui, Hawaii, USA, in the Pailolo and Auau Channels between the Hawaiian Islands of Maui, Molokai and Lanai (FIGURE 1). All of the deployments were on the inner shelf in water depths less than 11 m (FIGURE 2) in sediment-filled depressions. The seafloor sediment at all instrument locations is a well-sorted carbonate sand. All vessel operations, including mobilization and demobilization, were based out of Lahaina Harbor, West Maui, Hawaii.

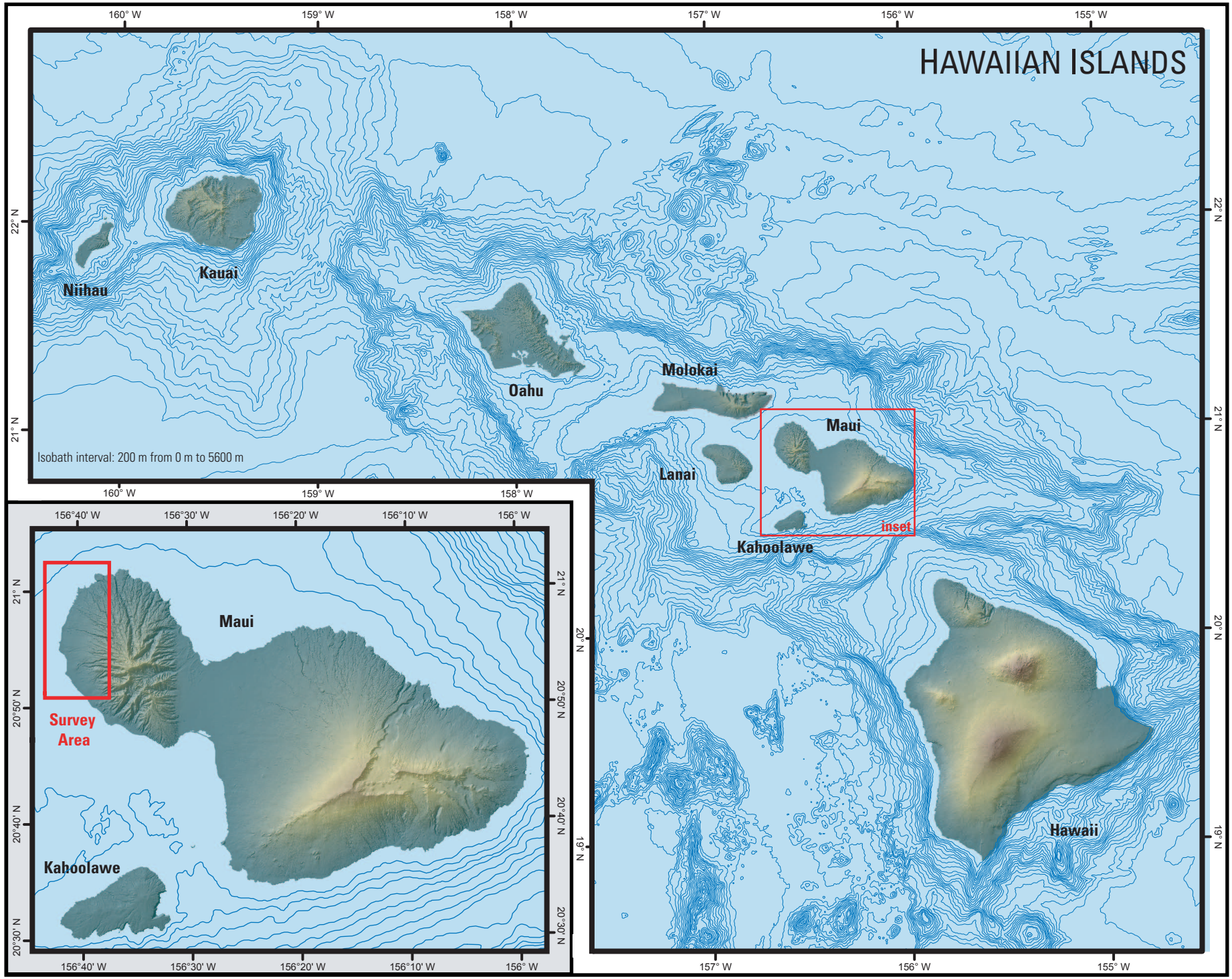

FIGURE 1. *Map of the study area location in the main Hawaiian Island chain.*

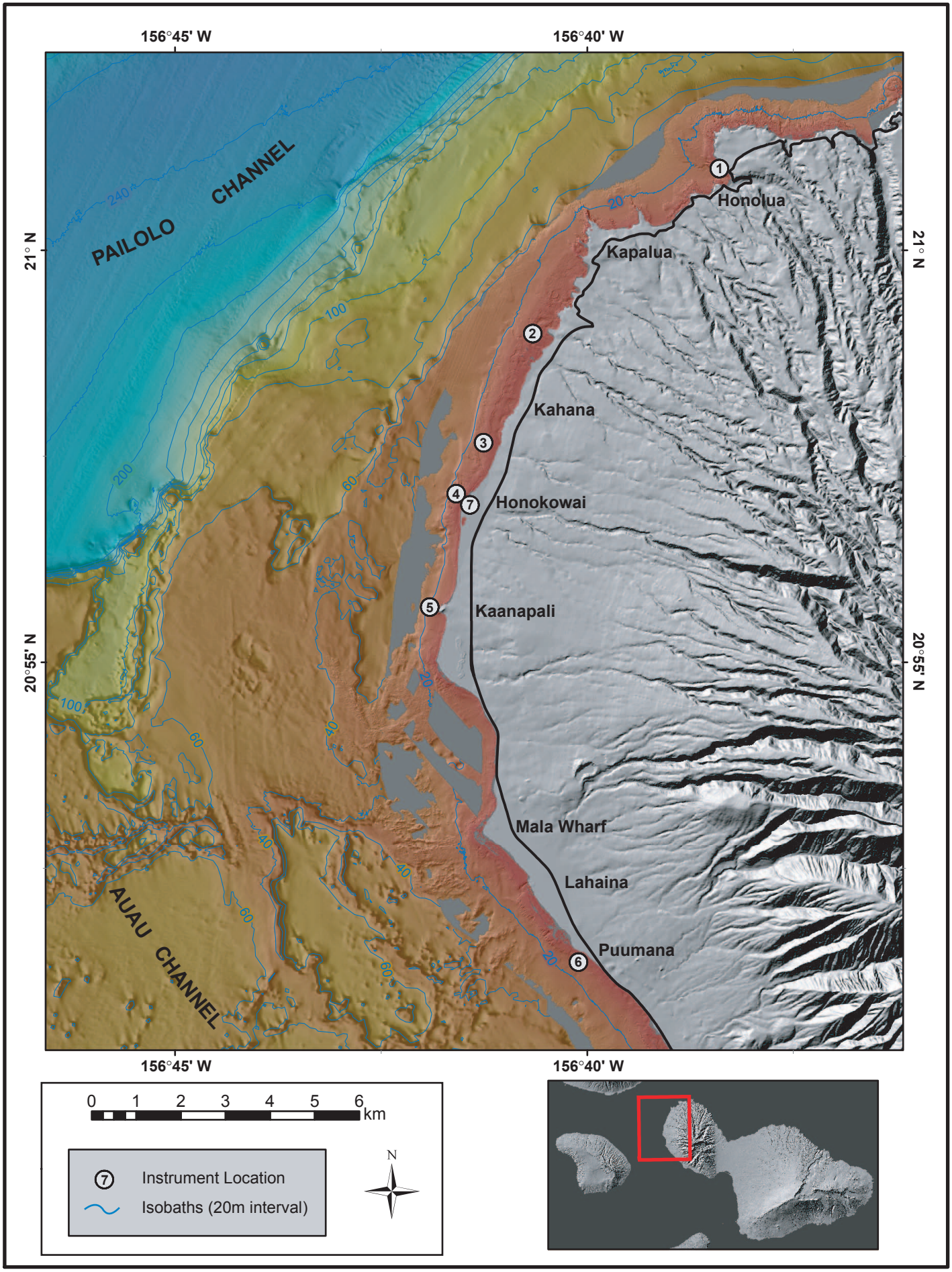

FIGURE 2. *Location of the instrument packages with nearshore bathymetry from SHOALS lidar data and digital elevation model (DEM) data of the terrestrial portion of the study area.*

OPERATIONS

This section provides information about the personnel, equipment and vessel used during the deployments. See TABLE 1 for a list of personnel involved in the experiment and TABLES 2 and 3 for complete listings of instrument and deployment information.

Scientific Party:

The scientific party for these deployments included at a minimum of three scientists from the USGS Coral Reef Project and one cooperating scientist from the University of Washington (UW). During instrument deployment and recovery operations, there was one vessel captain in addition to these scientists on board.

Equipment and Data Review:

The main instruments and sensors used to acquire hydrographic data during the experiment are listed in TABLE 2. The primary instruments were RD Instruments 600 kHz Workhorse Monitor upward-looking Acoustic Doppler Current Profilers (ADCP), which were used to collect vertical profiles of current velocity and acoustic backscatter data (FIGURE 3a).

Three other self-contained sensors were also deployed during this experiment: NIWA Dobie-A strain gauge pressure sensors (FIGURE 3b), Aquatec/Seapoint 200-TY self-logging optical backscatter (SLOBS) sensors and Seabird SBE-37SM Microcat conductivity-temperature (CT) sensors. These sensors collected single-point measurements on waves and tides, optical backscatter, and temperature and salinity, respectively. The instrument package deployment and recovery log is presented in TABLE 3. The instrument specifics and sampling schemes are listed in APPENDIX 1 and APPENDIX 2 for the ADCP profiler and other sensors, respectively.

Meteorologic data were acquired via a NovaLynx WS-16 weather station that was mounted on top of the Embassy Suites Hotel, Honokawai, to capture the meteorologic forcing during the experiment. Navigation equipment consisted of a hand-held WAAS-equipped GPS unit and a computer with positioning and mapping software. The positioning and mapping software enabled real-time GPS position data to be combined with images of previously collected high-resolution SHOALS lidar color-coded, shaded-relief bathymetry, GIS-generated 5 m isobaths and vertical aerial photographs of terrestrial portions of the maps. These systems made it possible to very accurately deploy the instruments in the same location and to recover them without the need for a surface float to mark the instruments' locations.

Research Platform:

The instrument deployments and recoveries were conducted using a leased vessel, the 28-ft-long *R/V Alyce C.*, owned and operated by Alyce C. Sport Fishing (FIGURE 3c). The *R/V Alyce C.* is a sport-fishing boat that was modified for scientific studies. While there are no laboratory compartments on *R/V Alyce C.*, the space below the bridge, the port beam and starboard quarterdeck were modified for instrument deployment and recovery. The port beam was used for instrument package deployment and recovery operations, which included the use of an electric winch and an overhead davit.

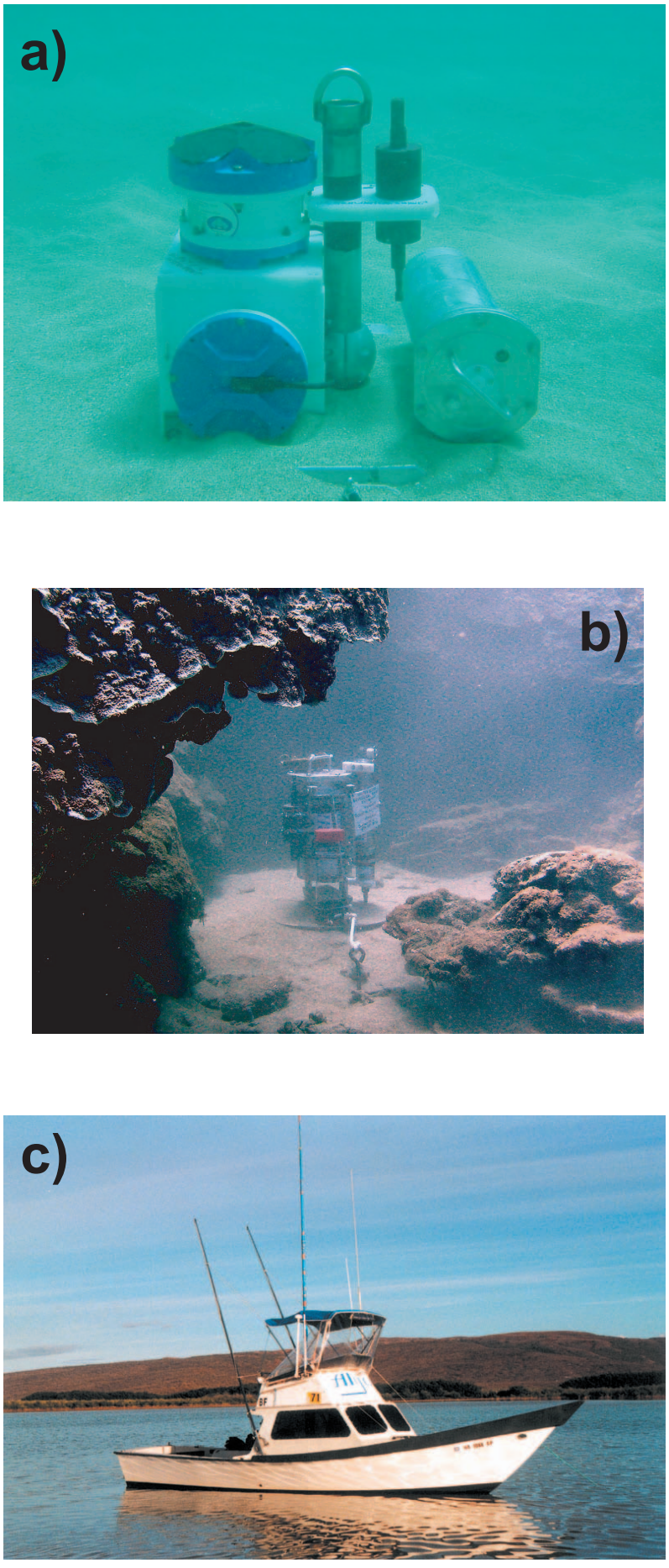

FIGURE 3. *Photographs of instrument packages and the deployment vessel. (a) View of the MiniPROBE instrument package on the seafloor along the 2 m isobath in a 2 m deep sediment-filled depression. (b) View of the MegaDOBIE instrument package on the seafloor along the 10 m isobath. (c) View of the R/V Alyce C.*

Deployment/Recovery Operations:

The instruments were deployed by attaching a removable bridle to the instrument package with a connecting line through the davit and down to the winch. The instruments were lowered to within a few meters of the seafloor, where scuba divers attached a lift bag and detached the lifting line. The divers then moved the instrument package into place, emplaced sand anchors into the seafloor and attached them to the instrument package using cables and turnbuckles. Sediment samples were collected from the seafloor and the height of the sensors above the seafloor were measured and recorded. The same procedures were employed during recovery operations.

DATA ACQUISITION AND QUALITY

Data were acquired 108 continuous days during the period from 06/28/2003 to 10/14/2003. More than 99% of the data from the ADCP profilers were recovered and the data quality was generally very high. The ADCP data near the surface displayed slightly lower correlation due to bubble interference with the transducers. This loss of data from the bins closest to the surface is common to most upward-looking ADCPs and was expected. The raw ADCP data were archived and copies of the data were post-processed to remove all “ghost” data from above the surface. All the data having a beam correlation below 70% were discarded for visualization and analysis. Post-processed data were saved and copies were desampled to hourly intervals to better visualize longer-term variability; these desampled copies of the data were also saved and archived. The acoustic backscatter data (ABS) is displayed as the amount of backscatter in dB above the minimum backscatter value or baseline observed during the record, which is interpreted to be clear water based on the co-located SLOBS data.

The Dobie data quality was generally very high except toward the end of the deployment when biofouling (biological growth) interfered with the pressure sensors’ operation. In some deployments, the instrument packages slowly settled due to wave-induced scour; this offset was easily identified (as abrupt offsetting increases in depth) and rectified, resulting in no distortion of the wave data. Most of the SLOBS and CT sensors, which are very susceptible to biofouling, incurred heavy biofouling, which resulted in some severely degraded data. The time periods of degraded data are denoted in the following plots as gray shaded regions and should not be interpreted as actual trends in the data. The statistics for all parameters presented in this report are calculated only for periods when the sensors were working properly or were not fouled (regions with a white background on the plots). Meteorologic data quality was excellent, with full data recovery and no apparent problems with the sensors.

RESULTS AND DISCUSSION

This section reviews the data collected by both systems during the deployments and addresses the significance of the findings to better understanding the local oceanographic conditions in the study area.

Meteorology

The data from the meteorologic station at Honokawai are shown in FIGURE 4. Daily insolation-induced Trade wind intensification is evident in the anemometer record. While the mean ± one standard deviation of wind speeds was 5.87 ± 3.29 m/sec, the daily afternoon wind speeds averaged 10-12 m/sec. The mean ± one standard deviation of precipitation was 0.011 ± 0.040 cm; precipitation, like the winds, displayed a daily modification related to orographic effects due to Trade wind intensification. Conversely, when the Trade winds slack, precipitation was generally not observed. The mean ± one standard deviation of air temperature was 26.3 ± 2.1 °C. Air temperature did not show any long-term trend but a 2-4 °C daily increase in air temperature due to insolation is evident. The peaks in air temperature are strongly correlated to periods when the Trade winds waned, reducing surface cooling and thus causing near-surface air temperatures to rise.

Tides

The deployments encompassed more than 6 complete Spring-Neap tidal cycles (FIGURE 5a). The tides off West Maui are of the mixed, semi-diurnal type with two uneven high tides and two uneven low tides per day; thus the tides change just over every 6 hours. The mean daily tidal range is roughly 0.6 m, while the minimum and maximum daily tidal ranges are 0.4 m and 1.0 m, respectively.

Waves

The waves that impacted West Maui during the course of the experiment are shown in FIGURES 5-7. Wave heights (*Hsig*) ranged from 0.05-0.95 m and wave periods (*Tdom*) varied from 4-22 sec; peak wave-induced near-bed shear stresses (*taub*) ranged from 0.03-0.97 N/m^2. Clearly evident in the data is the gradual increase in wave height and period from the northern end of the study area (FIGURE 5) towards the southern end (FIGURE 7) throughout the study (compare subplots “b” and “e” in FIGURES 5-7). This trend demonstrates the greater influence of long period Southern swell during the Northern Hemisphere’s summer (Southern Hemisphere’s winter) when intense storms in the Southern Ocean generate large waves that propagate north to the Hawaiian Islands. The Southern swell appears to greatly influence the near-bed wave-induced shear stresses up to Black Rock Point at Kaanapali (instrument location #5 in FIGURE 2). This point has been referred to by natives as a significant region oceanographically along West Maui, with it being the dividing point between the Northern West Maui and Southern West Maui. Specific wave events like the one the impacted the shoreline between Julian Days 182-188 show that sometimes Southern swell energy can propagate past Black Rock Point at Kaanapali to Northern Kahana. Subsequent observations made during the 2003-2004 winter (Storlazzi, unpublished field notes) show that the largest waves observed along West Maui are observed in Honolua Bay during the winter months; however, during the summer months when this study was conducted, the smallest waves were observed at that site.

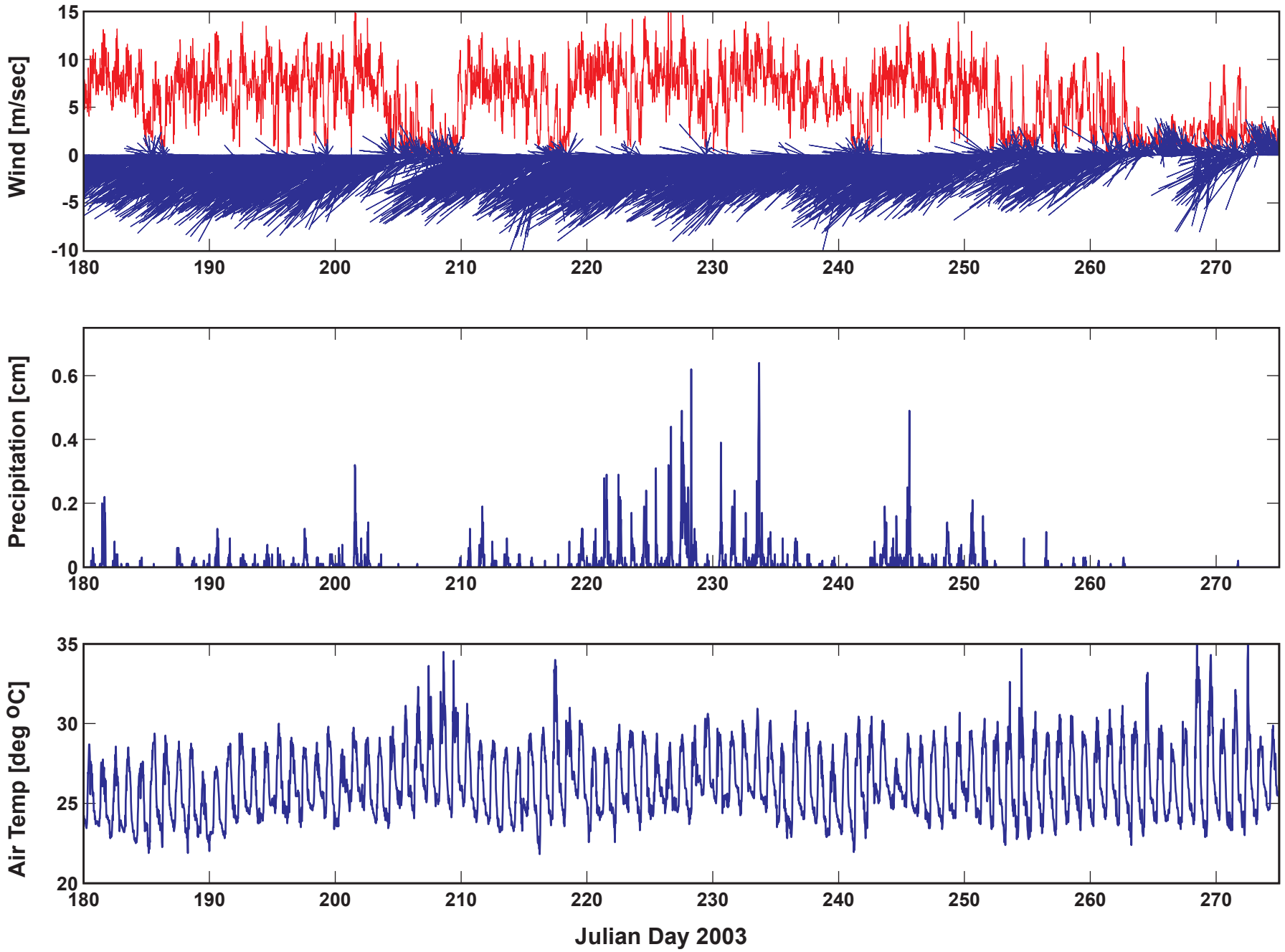

FIGURE 4. *Meteorologic forcing during the experiment. Daily insolation-induced Trade wind intensification is evident in the wind records, as is the much lower velocity winds out to the north. Precipitation, like the winds, shows a daily modification related to orographic effects due to Trade wind intensification; conversely, when the Trade winds slack, precipitation was generally not observed. Air temperature did not show any long-term trend but a 4-5 ^{O}C daily increase in air temperature due to insolation is evident.*

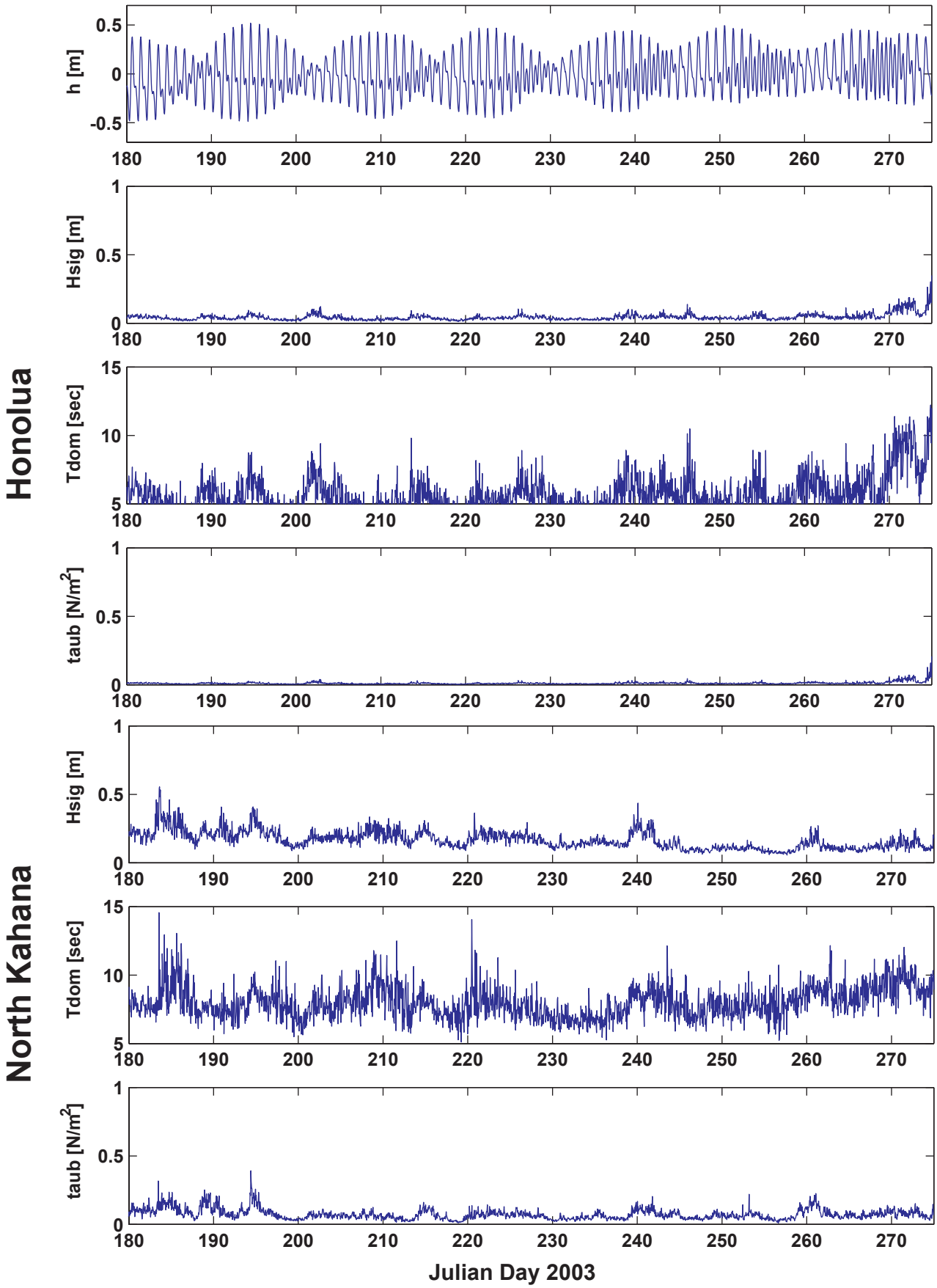

FIGURE 5. *Tide and wave data from the northern part of the study area. Top panel: Tidal height. Next three panels: Significant wave height (Hsig), dominant wave period (Tdom) and peak wave-induced near-bed shear stress (taub) off Honolua. Bottom three panels: Significant wave height (Hsig), dominant wave period (Tdom) and peak wave-induced near-bed shear stress (taub) off North Kahana. Note the much lower wave heights, periods and associated shear stresses off Honolua, which is protected from North Pacific swell and northeast Trade wind waves by the headlands to either side of the bay. North Kahana is less well protected and thus receives more refracted wave energy from the north and northeast.*

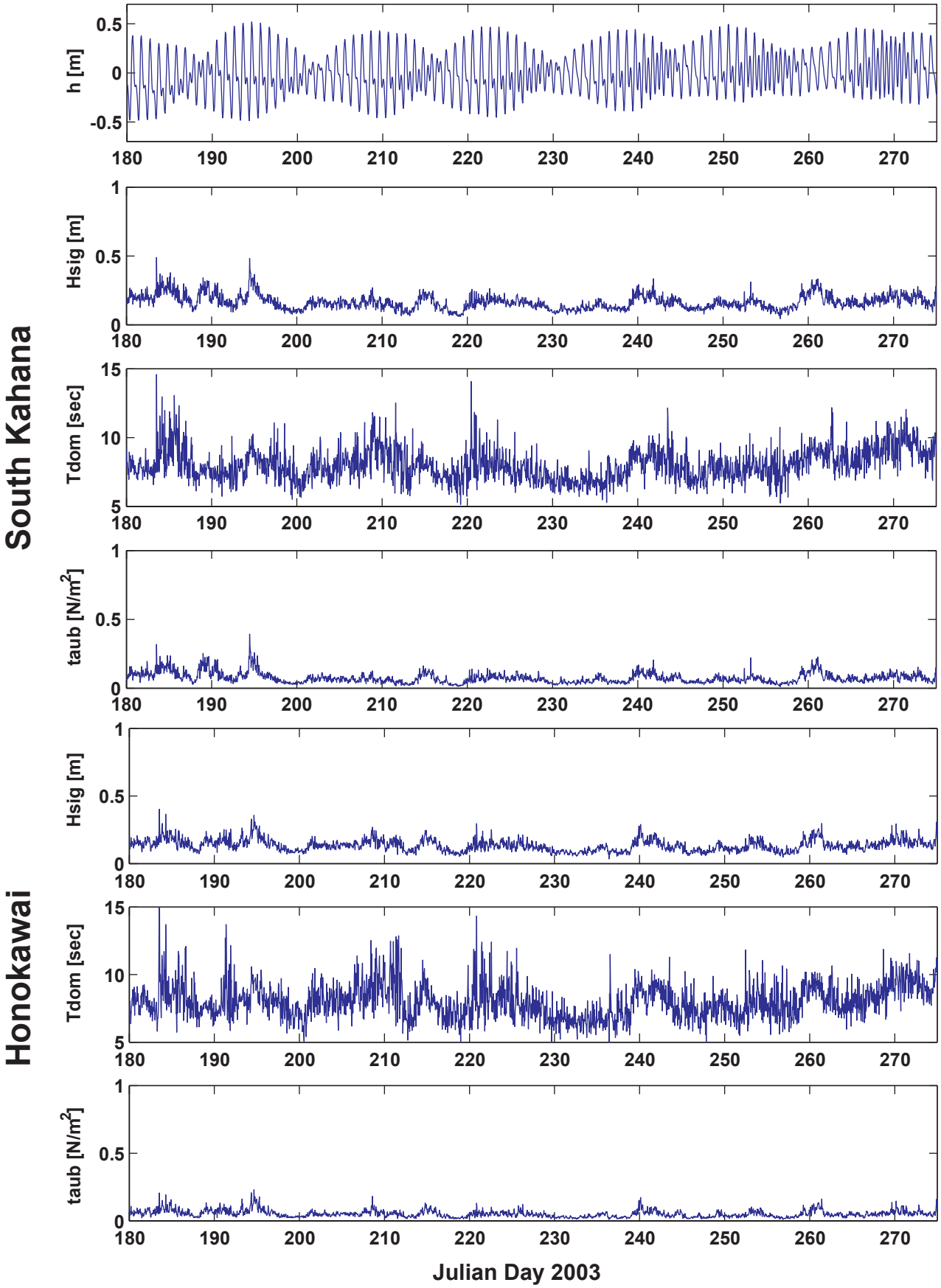

FIGURE 6. *Tide and wave data from the central part of the study area. Top panel: Tidal height. Next three panels: Significant wave height (Hsig), dominant wave period (Tdom) and peak wave-induced near-bed shear stress (taub) off South Kahana. Bottom three panels: Significant wave height (Hsig), dominant wave period (Tdom) and peak wave-induced near-bed shear stress (taub) off Honokawai. The wave heights are shear stresses are slightly lower at Honokawai than off South Kahana; however, the wave periods are similar, suggesting that both regions are dominated by waves out of the north. Honokawai, being further south, thus receives less wave energy than South Kahana and North Kahana (FIGURE 5).*

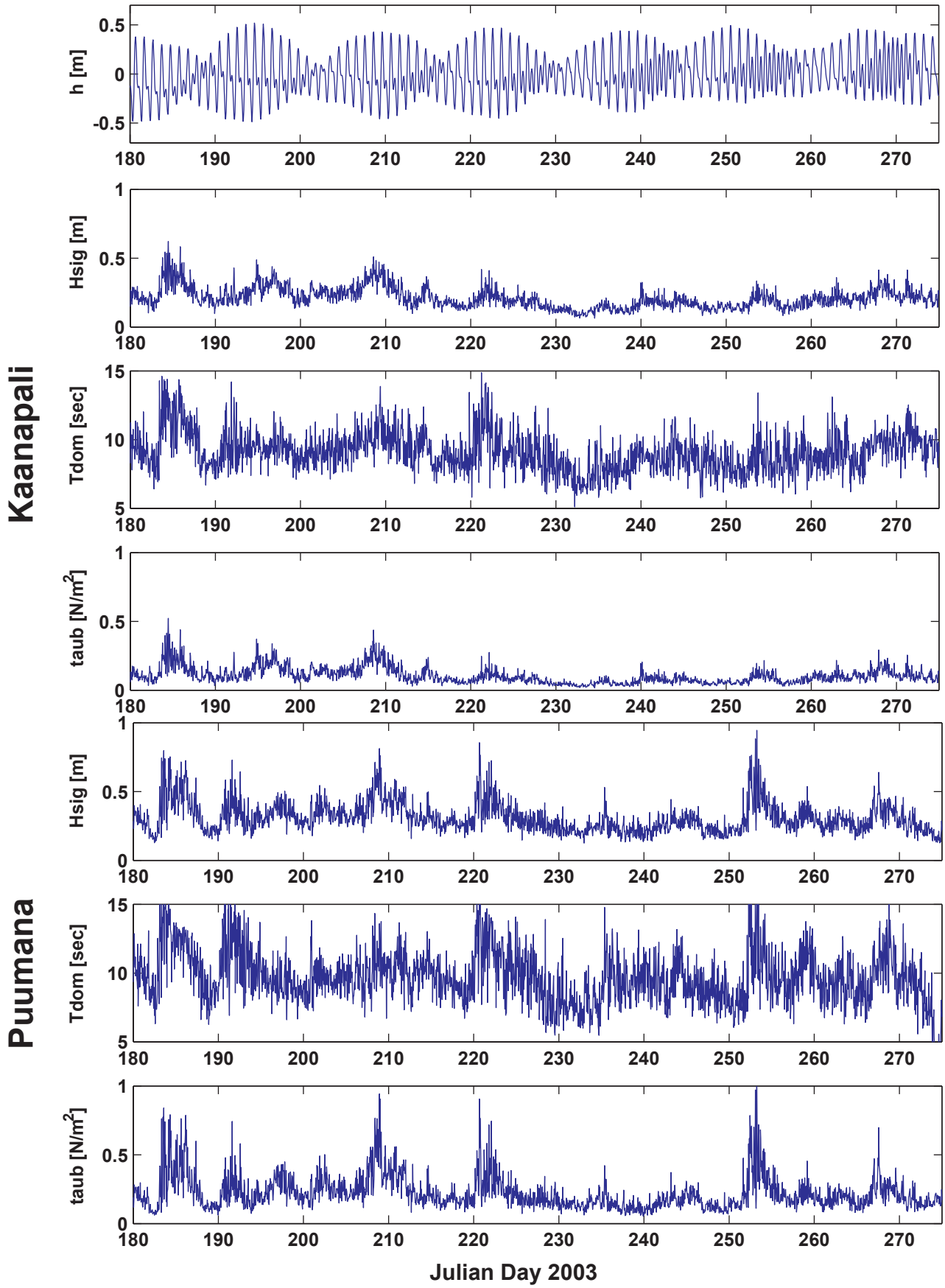

FIGURE 7. *Tide and wave data from the southern part of the study area. Top panel: Tidal height. Next three panels: Significant wave height (Hsig), dominant wave period (Tdom) and peak wave-induced near-bed shear stress (taub) off Kaanapali. Bottom three panels: Significant wave height (Hsig), dominant wave period (Tdom) and peak wave-induced near-bed shear stress (taub) off Puumana. Puumana, which has a southern exposure, is impacted by larger, longer-period south swell commonly observed during the summer months. Kaanapali, which faces due west, is impacted by waves from both the north (FIGURES 5 and 6) and south.*

Water Column Properties

The water column properties that were collected included variations in temperature (ºC), salinity (PSU), optical backscatter (NTU) and acoustic backscatter (dB).

***Temperature*:**

Water temperature generally increased from north to south in the study area, as shown in FIGURES 8-10 and TABLE 5. Over the period of study, the water temperatures along the study area ranged between 25 °C and 28 °C, with a mean temperature ± one standard deviation of 26.41 ± 0.40 °C. At all sites, the water typically warmed 0.2-0.4 °C during the day due to insolation. Over time scales longer than tidal periods (>24 hours), we observed long-term warming similar to the air temperature record from the weather station (FIGURE 4). These appear to be driven by reduced wind speeds as the Trade winds wane and possibly by increased insolation due to the absence of Trade wind-induced orographic clouds. Conversely, longer-term cooling trends tended to correspond to periods following precipitation. These cooling trends might be due to cooler freshwater discharge from streams or via submarine groundwater discharge causing the general cooling observed along the 10 m isobath following precipitation events. At tidal periods (12-24 hours), water temperatures typically increased when the tidal elevation fell. This is likely due to water warmed in the shallows closer to the shoreline being advected obliquely offshore out past the deeper instrument packages along the 10 m isobath. The cooling during rising tides is likely due to the excursion of deeper, cooler water from the Auau and Pailolo Channels up to the 10 m isobath where the instruments were located.

Another very interesting temperature pattern was often observed in the high-frequency (every 4 min) temperature records (not shown). When the Trade winds blew consistently, roughly once per day, very rapid (typically <16-32 min) warming or cooling was observed. The water temperature typically changed by more than 0.5 °C and frequently by more than 1.0 °C. These rapid changes in water temperature occurred during all but the spring phases (new and full moon) of the lunar tidal cycle and during all phases (low, rising, high and falling) of the diurnal tidal cycle. These patterns were also observed over 15 months of observations off North Kahana in 2002 and are discussed in greater detail by Storlazzi and Jaffe (2003).

***Salinity*:**

Over the period of study, the water salinities at the sites along the study area ranged between 30.1 PSU and 35.2 PSU, with a mean salinity ± one standard deviation of 35.67 ± 0.21 PSU as shown in FIGURE 8 and TABLE 5. A general decrease in salinity was observed at all three stations over the first 38 days of the deployment (Julian Days 180-218). Over tidal (12-24 hours) timescales, higher salinity water typically moved onshore with the rising tide and lower salinity water moved offshore with the falling tide. Numerous large, low-salinity excursions are evident in the salinity time series and either occur concurrently with or follow soon after precipitation events (FIGURE 4). The causes of these infrequent low salinity pulses are not yet fully understood. They are roughly correlated in time with both offshore flow and precipitation events. The low salinity pulses may have been caused by freshwater

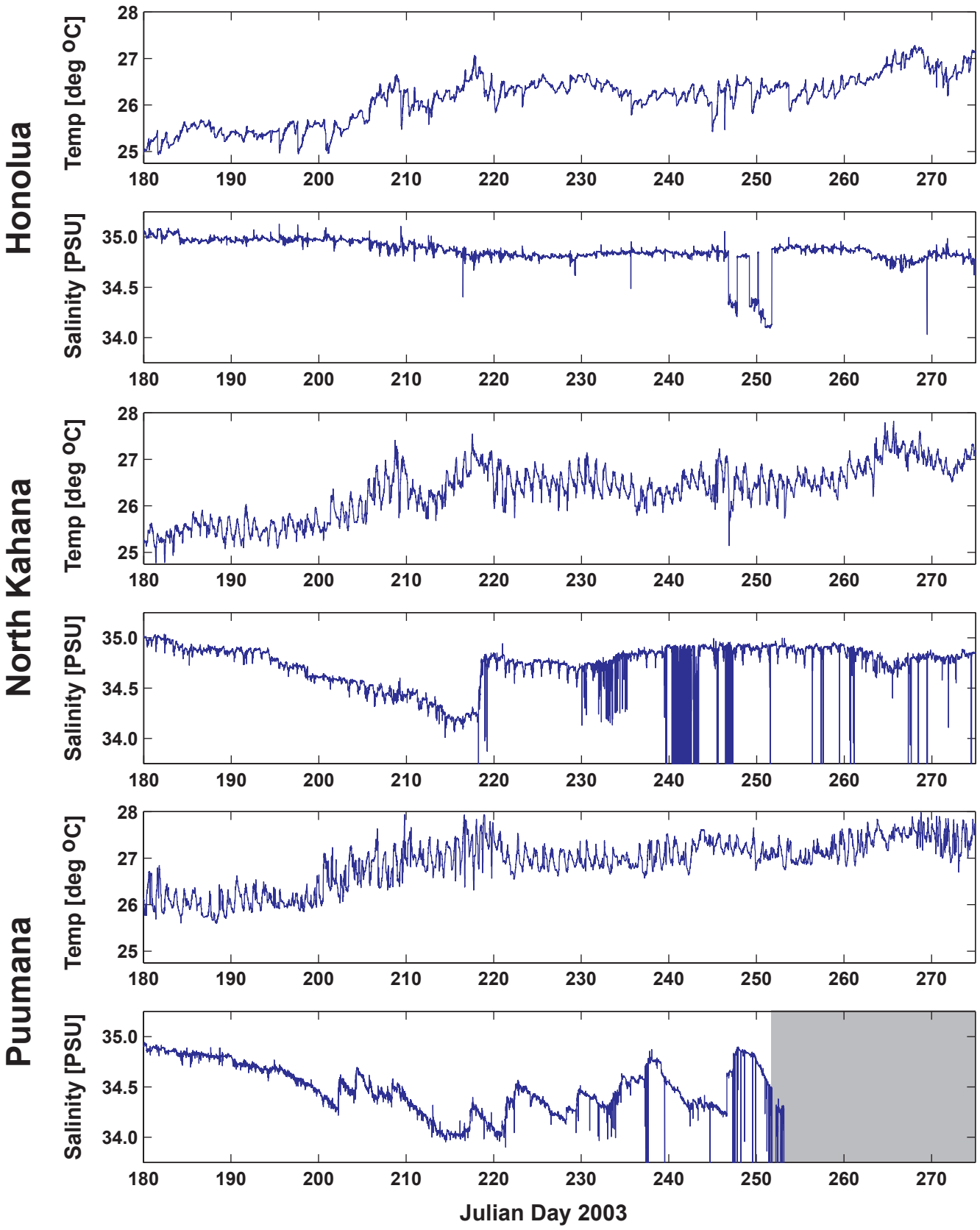

FIGURE 8. *Hourly mean near-bed water temperatures in the study area. Top panels: temperature and salinity from off Honolua. Middle panels: temperature and salinity from off North Kahana. Bottom panels: temperature and salinity from off Puumana. Gray areas denote periods of sensor malfunctions. Temperature at all sites increased throughout the summer due to insolation. Note the semi-diurnal 0.25-0.50 ^{O}C fluctuations due to internal tides and the much lower daily variability off Honolua.*

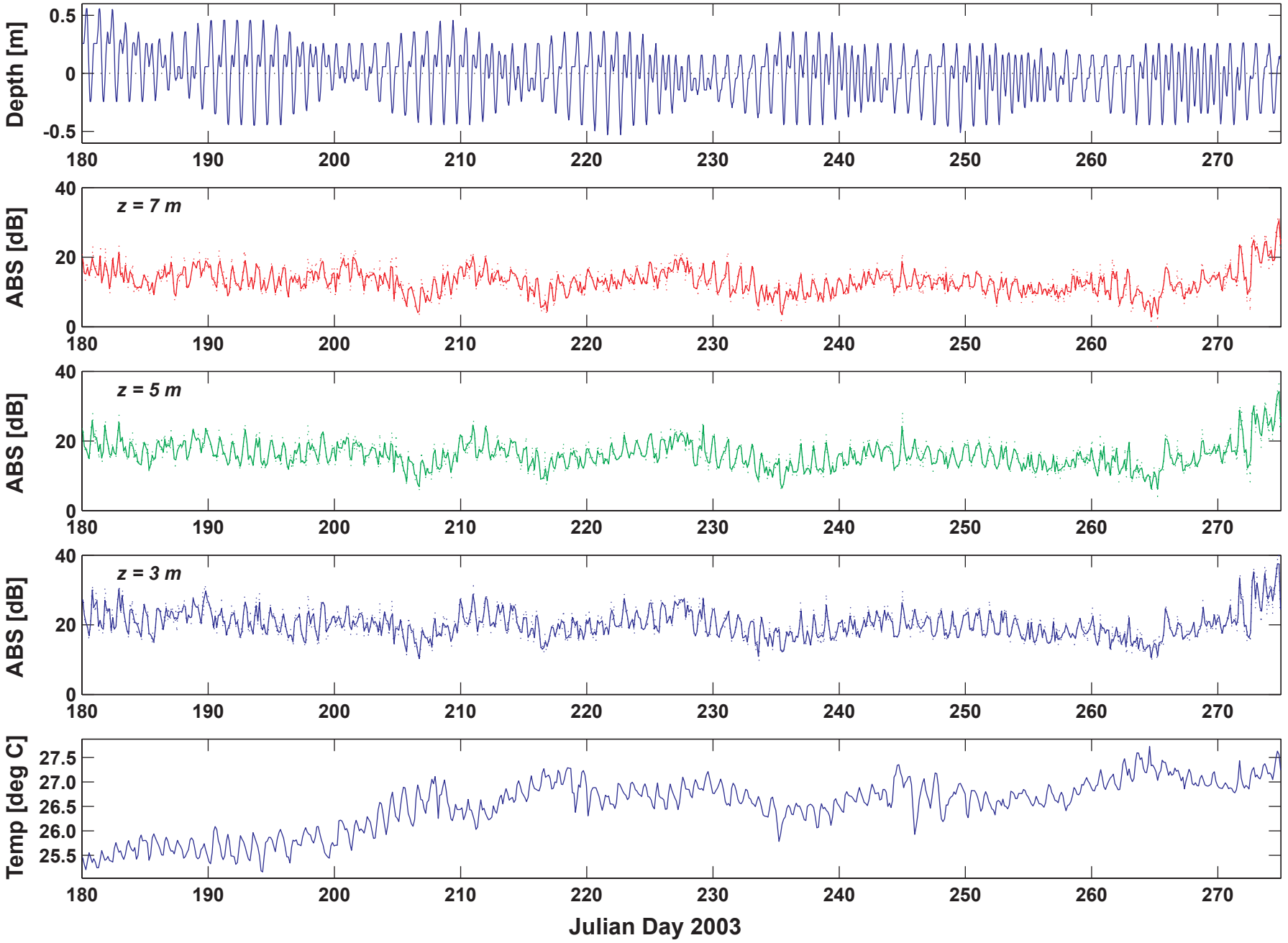

FIGURE 9. *Tidal height, acoustic backscatter (ABS) and near-bed water temperature at the South Kahana site. The acoustic backscatter is shown for three elevations above the bed: 7 m, 5 m and 3 m in red, green and blue, respectively. Semi-diurnal fluctuations are evident in the acoustic backscatter and temperature data, with higher temperatures and acoustic backscatter during the falling tides. Acoustic backscatter is also positively correlated with wave-induced near-bed shear stress at subtidal (>36 hours) frequencies (FIGURE 6). The acoustic backscatter at all three elevations above the bed is slightly higher off South Kahana than further south off Honokawai (FIGURE 10).*

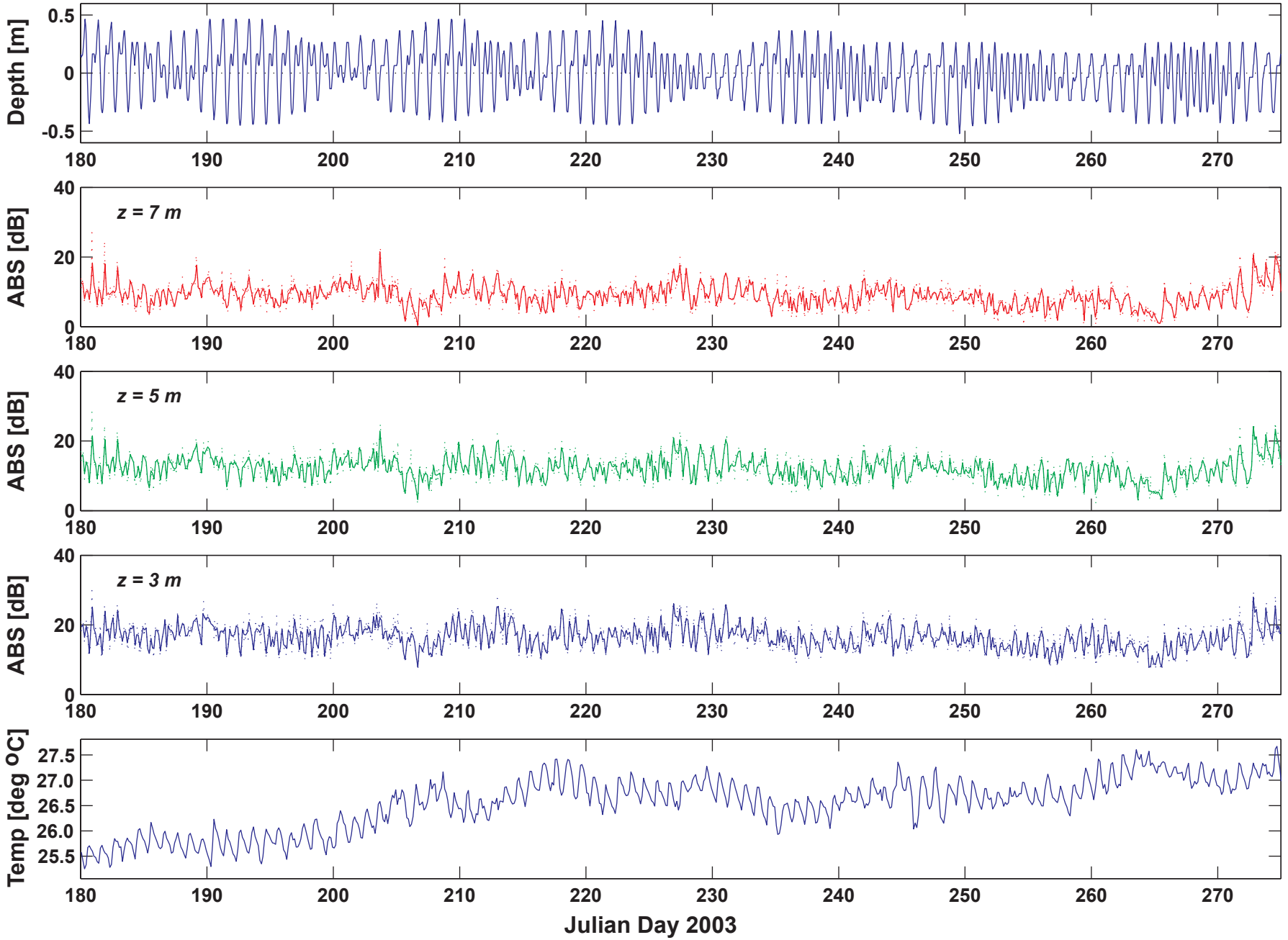

FIGURE 10. *Tidal height, acoustic backscatter (ABS) and near-bed water temperature at the Honokawai site. The acoustic backscatter is shown for three elevations above the bed: 7 m, 5 m and 3 m in red, green and blue, respectively. Semi-diurnal fluctuations are evident in the acoustic backscatter and temperature data, with higher temperatures and acoustic backscatter during the falling tides. Acoustic backscatter is also positively correlated with wave-induced near-bed shear stress at subtidal (>36 hours) frequencies (FIGURE 6). Temperature variability is slightly higher off Honokawai than to the north off South Kahana (FIGURE 9).*

discharge from onshore drainages or fresh groundwater diffusing out of the reef, at either short-term or long-term rates, or some other process related to water circulation. We did not have salinity sensors inshore of the 10 m sites, and cannot confirm a hypothesis of freshwater input.

***Acoustic and Optical Backscatter*:**

Overall, the instruments off South Kahana (FIGURE 9) recorded greater acoustic backscatter and turbidity than those off Honokawai (FIGURE 10). Acoustic backscatter, a proxy for particulate matter in the water column, was generally both more intense and more variable closer to the bed than higher in the water column at both instrument sites. The acoustic backscatter is well correlated at subtidal (> 36 hours) time scales with wave-induced near-bed shear stress (FIGURE 6). Over shorter (< 26 hours) timescales, acoustic backscatter appears linked to the tides, with lower backscatter observed during rising tides and higher backscatter during falling tides. This suggests that as water drains off the shallower portion of the reef inshore of the instruments, it might carry with it particulate matter that interacts with the acoustic beams. Similar high-frequency variability can be observed in the SLOBS data (FIGURE 11). The measured turbidity 0.2 m above the bed at the sites along the 10 m isobath ranged between 0.0 NTU and 15 NTU, with a mean turbidity ± one standard deviation of 0.88 ± 0.44 NTU, 0.91 ± 1.43 NTU and 0.79 ± 0.13 NTU for the Honolua, South Kahana and Honokawai sites, respectively. The highest turbidity values recorded by the SLOBS were not clearly correlated to any forcing mechanism such as waves, tides or winds, unlike the acoustic backscatter data. On a side note, both scuba divers and sea turtles have often been observed during previous instrument deployments and reconnaissance dives at the sites where the SLOBS were deployed and may have interfered with the optical beam. At this time, however, we cannot determine what caused the high turbidity values recorded by the SLOBS at the Honolua, South Kahana and Honokawai instrument sites.

Currents

Most of the daily variability in current speed and direction at the study sites are due to the tides. As the tide rises (floods), currents off West Maui flow to the northwest roughly parallel to shore; conversely, as the tides fall (ebb), the currents flow to the southwest roughly parallel to shore. This pattern is set by the local of the tidal node (amphidrome) to the west of the Hawaiian Island chain and the counter-clockwise sweep of the tidal bulge around the amphidromic point. Mean tidal current speeds ± one standard deviation at the South Kahana site were 0.18 ± 0.47 m/sec close to the surface and 0.11 ± 0.07 m/sec close to the sea floor (FIGURE 12). Mean tidal current speeds ± one standard deviation close to the surface at the Honokawai site were roughly 28% lower (0.13 ± 0.18 m/sec) and more than 45% lower close to the sea floor (0.06 ± 0.04 m/sec, FIGURE 13). The magnitude of the tidal currents is driven by the lunar tidal cycle, with the highest tidal current speeds occurring during the spring tides (new and full moons) and the weakest during the neap tides (quarter moons). Overall, the tidal currents are faster and more consistent in the alongshore direction at the South Kahana site than along the Honokawai site (FIGURE 14). While the rising and falling tidal currents off South Kahana are roughly opposite (180°) from one another, the falling

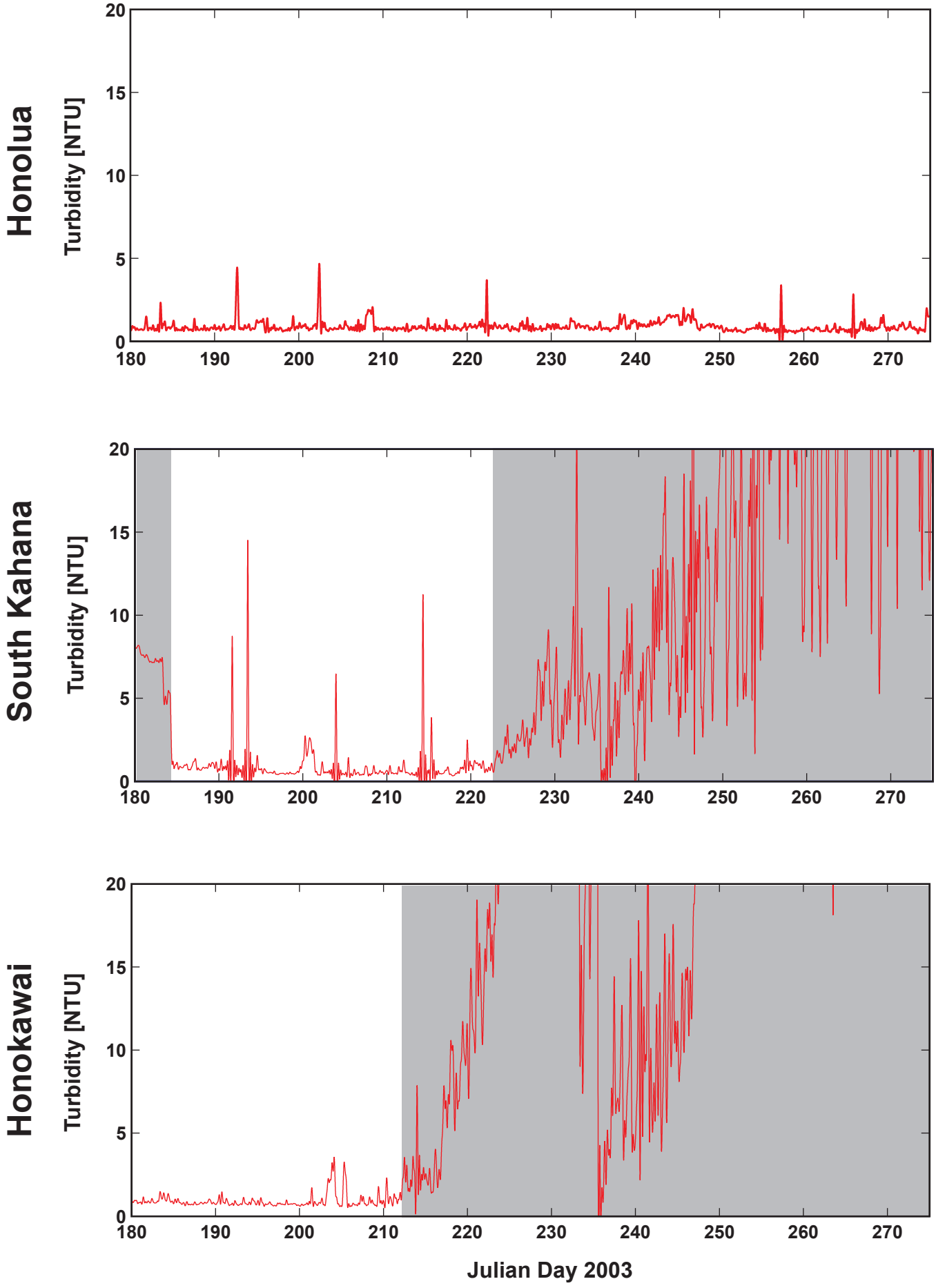

FIGURE 11. *Hourly mean near-bed turbidity data in the study area. Gray regions denote period of biofouling or infra-red beam obstruction. There is no clear correlation between the different sites or with the winds or waves.*

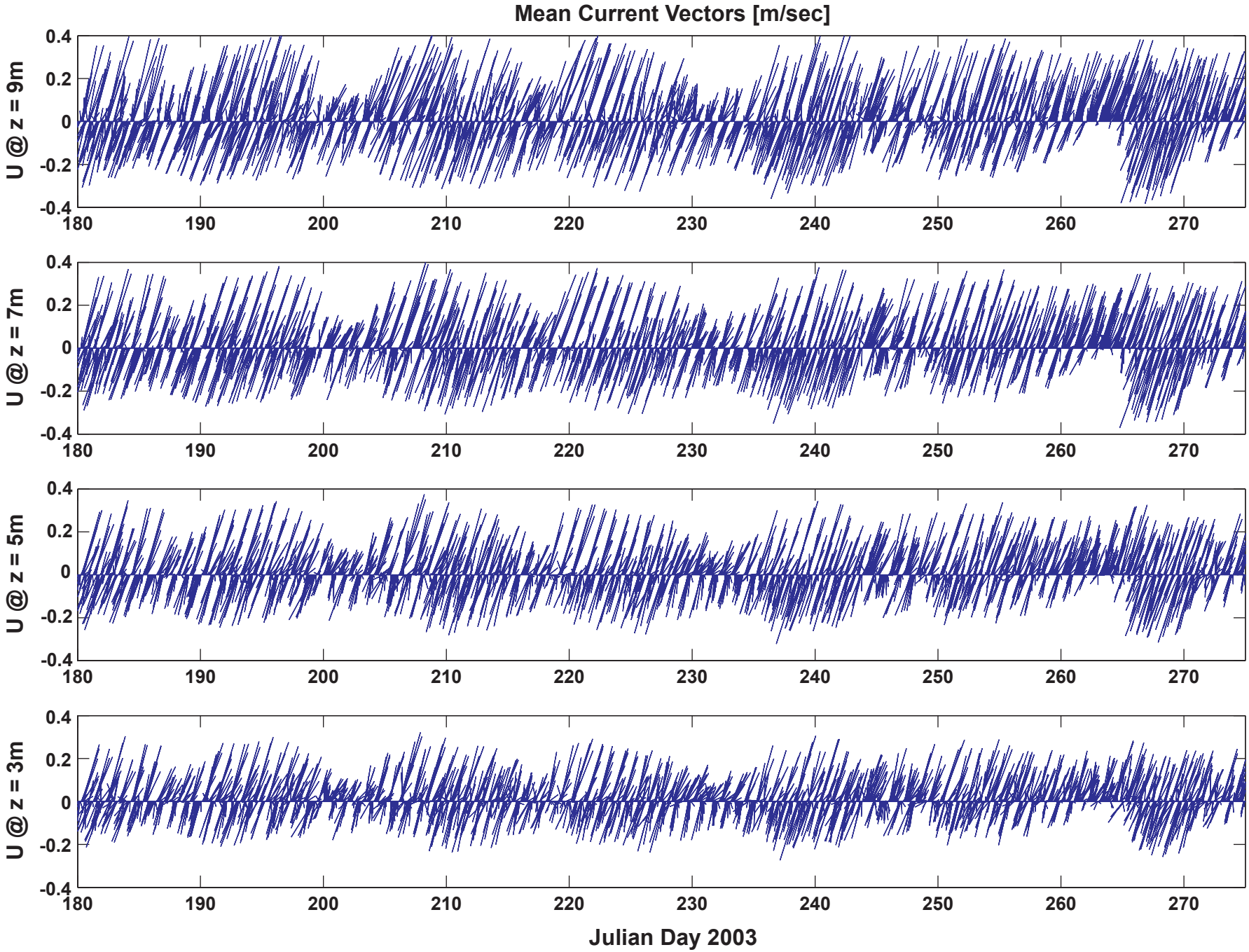

FIGURE 12. *Hourly mean current speeds and directions at the South Kahana site for different heights above the sea floor. Flow is dominated by alongshore tidal currents. During the periods when the Trade winds blow consistently, there is little net flow (i.e.- JD 220-230). When the Trade winds become more variable or weaken, however, net flow at the site is to the northeast (i.e.- JD 262-266). Current speeds are generally 0.05-0.10 m/sec greater off South Kahana than to the south off Honokawai (FIGURE 13).*

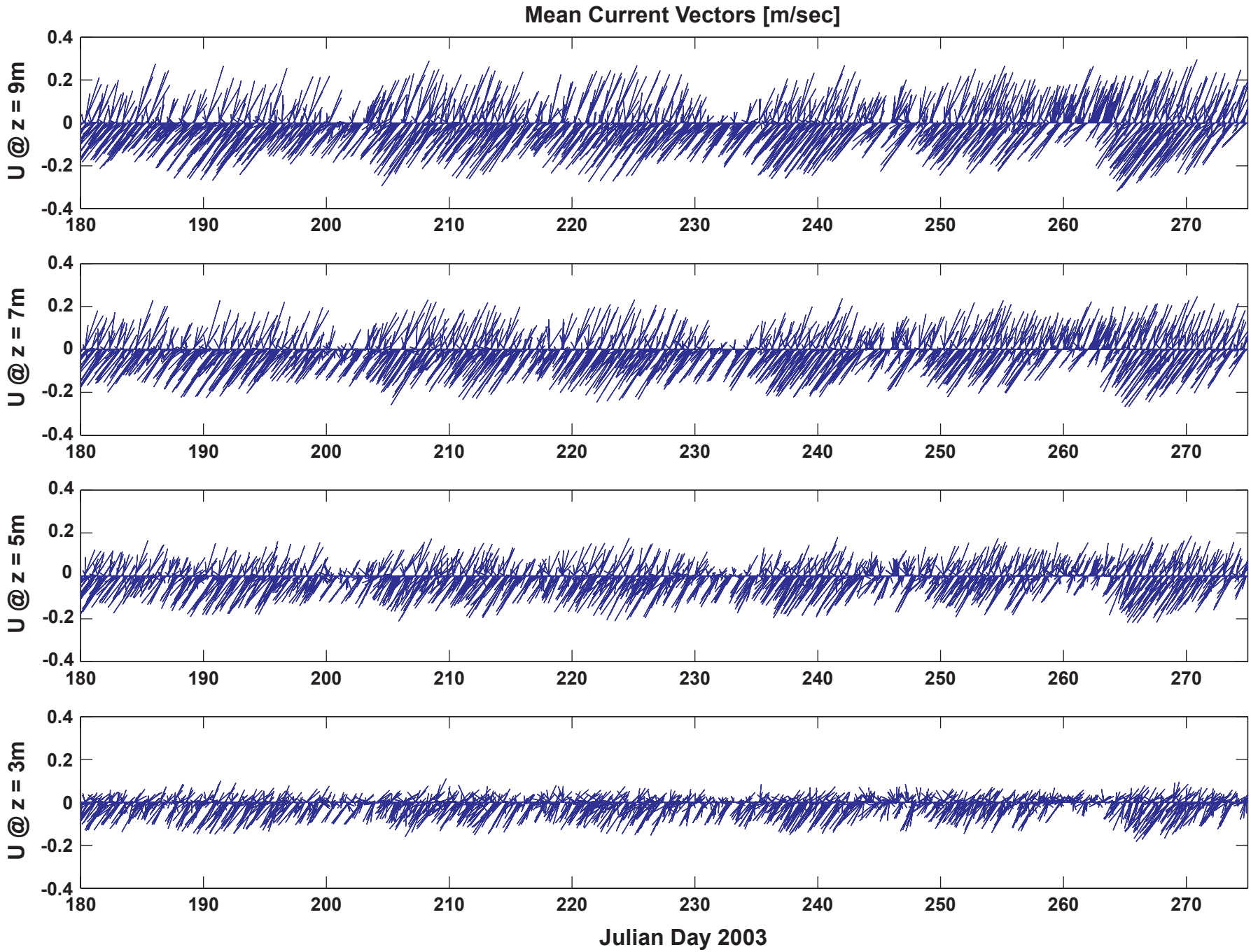

FIGURE 13. *Hourly mean current speeds and directions at the Honokawai site for different heights above the sea floor. Flow is dominated by alongshore tidal currents. During the periods when the Trade winds blow consistently, there is little net flow near the surface; under the same conditions near the bed, however, net flow is to the south (i.e.- JD 220-230). When the Trade winds become more variable or weaken, however, net flow near the surface at the site is to the northeast while near the bed under these conditions there is little net flow (i.e.- JD 262-266).*

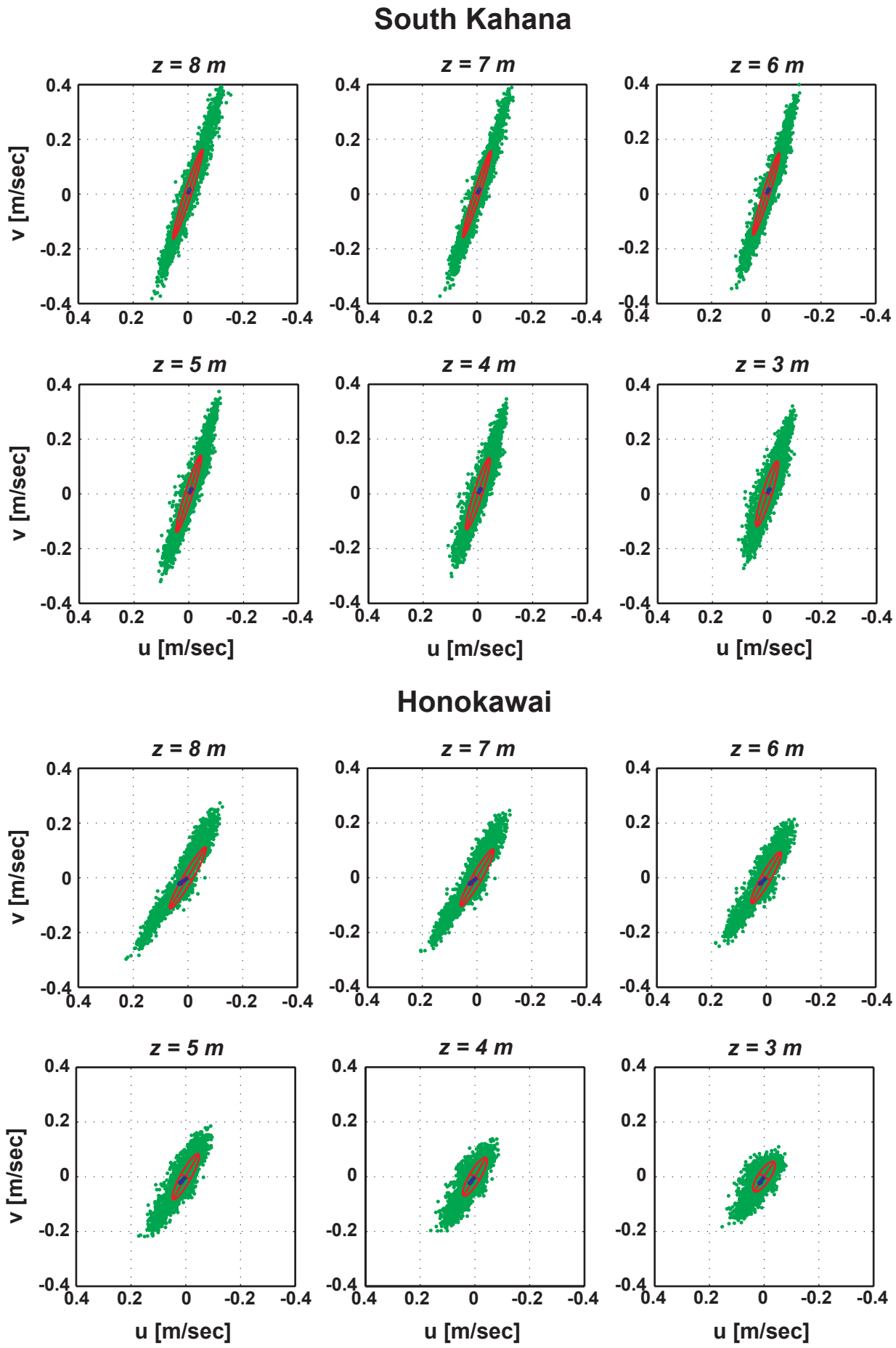

FIGURE 14. *Principal axes of flow at the South Kahana and Honokawai sites at different elevations above the sea floor. Each green dot displays the easterly (u) and northerly (v) current speed in map view of a single current measurement. The red ellipses denote the major (longer) and minor (shorter) axes of flow, with the major axis of flow being oriented roughly shore parallel. Note the different orientations in the principal axes of flow between the sites and the different orientation of the observations of southerly (-v) flow at the Honokawai site as compared to the observations of northerly flow (+v), suggesting bathymetric steering of currents by the Honokawai headland.*

tidal currents are oriented further offshore to the west. This might be due to the presence of a slight embayment between South Kahana and Honokawai that could cause the falling tidal current to be bathymetrically steered offshore when it interacts with the headland at Honokawai. This is the first time the authors have ever observed rising and falling tidal currents not oriented along the same horizontal axis in Hawaii or along the US West Coast.

The dominant factor other than tides at these sites driving flow are the winds. When the Trade winds blow at 5-15 m/sec to the southwest, as they typically do during most of the year (FIGURE 4), they force water in the Pailolo Channel between Maui and Molokai to the southwest (Storlazzi and Jaffe, 2003). Under normal Trade wind conditions, there was very little net alongshore flow at the South Kahana site. Net flow off the Honokawai site under the same conditions, however, was to the south, showing that there is a region of flow divergence between the South Kahana and Honokawai sites. When the Trade winds decrease in strength or are replaced by winds out of the south or west, as often occurs throughout the year and most frequently during the fall and winter months, we observed net flow to the northeast at both site along the 10 m isobath (FIGURE 12-13). This suggests that there may be some type of large-scale relaxation that occurs when the Trade winds decrease in strength, with the water that has been piled up by Trade winds in the channels between Maui, Molokai, Lanai and Kahoolawe (the Maui Nui group) being relaxed and flowing back out through the Pailolo Channel. Over the course of the entire deployment, projected net flow at the South Kahana site for all depths was to the north while net flow at the Honokawai site for all depths was to the south, again displaying the divergence in flow between these two sites (FIGURE 15). We do not have information at this time that indicates which process or combination of processes is responsible for the observed northeasterly flow when the Trade winds wane nor the cause of the divergence between the South Kahana and Honokawai sites.

Projected Coral Larvae Fluxes:

The projected spawning dates (E. Brown, personal communication) for the reef-building coral *Montipora capitata* off Hawaii during the 2003 summer were, with Julian Days 2003 in parentheses: June 30-July 2 (JD 181-183), July 29-July 31 (JD 210-212) and August 27-August 29 (JD 239-241). A series of 48-hour progressive vector diagrams of projected cumulative flow during these *Montipora capitata* spawning events off West Maui are shown in FIGURES 16-18. These data show projected surface particle trajectories over a 48-hour period starting at 21:00 hours on the specified dates. The buoyant lipid layer that covers the developing coral planula takes more than 24 hours to dissolve, causing the planula to sink and settle on the sea floor, so we assumed the majority of the planula could be carried by the currents for at least 36-48 hours before settlement occurred. These types of calculations make the assumption that the flow measured at the instrument site is uniform alongshore, which is rarely the case, often resulting in improbable tracks, i.e.- tracks that cross the shoreline. These calculations, therefore, can be used to determine the general direction and pattern of coral larval dispersal from the two main study sites off South Kahana and Honokawai. In general, they show that there was little net alongshore flow off the South Kahana site (dashed lines), suggesting that coral larvae released from the reefs at this location were

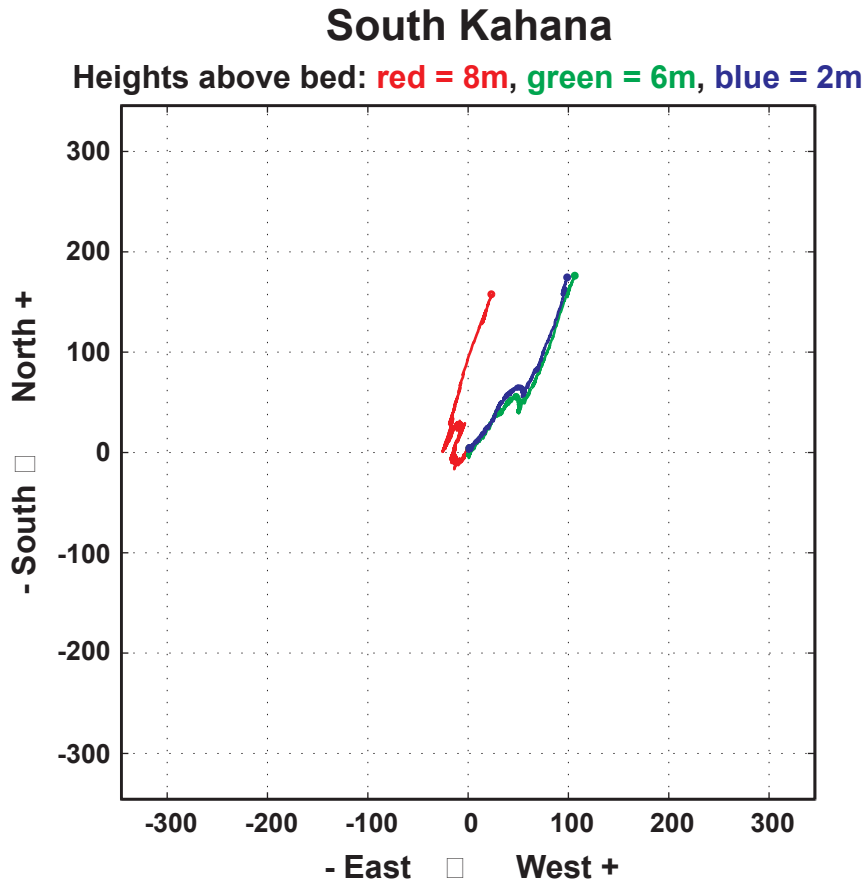

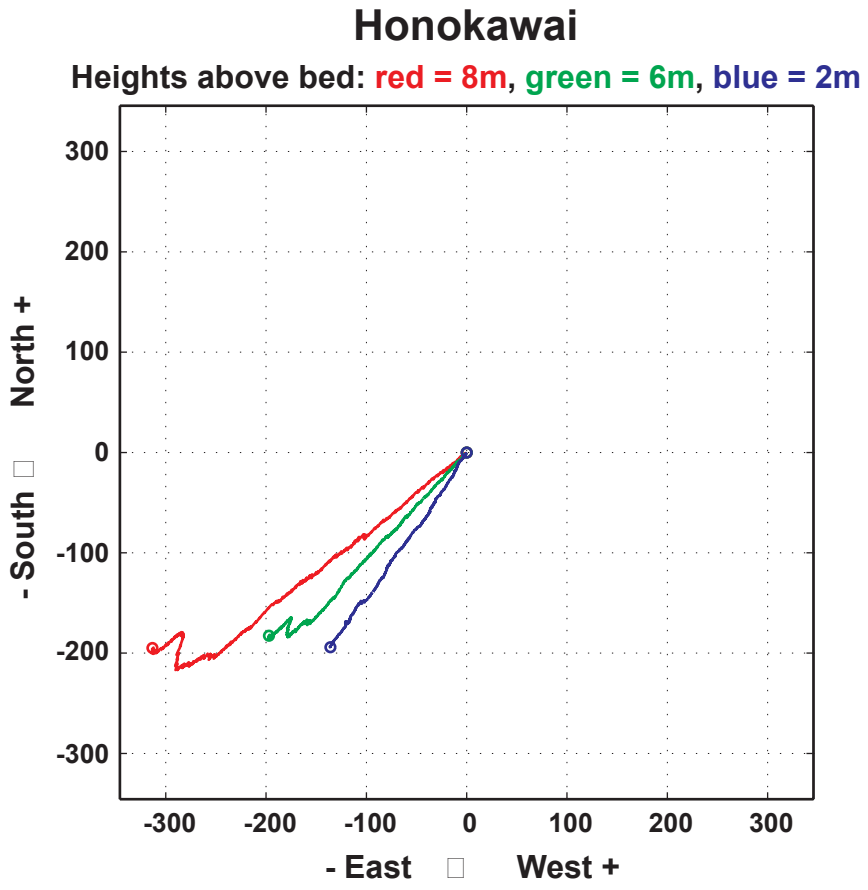

FIGURE 15. *Progressive vector diagram of projected cumulative flow for different elevations above the sea floor at the South Kahana and Honokawai sites. The distances are in units of kilometers. These calculations make the assumption that the flow measured at the instrument site is uniform alongshore, which is rarely the case. Note not only the different directions of net projected flow at the two sites but also the relative net projected distances of flow relative to the observed current speeds shown in FIGURES 12-13.*

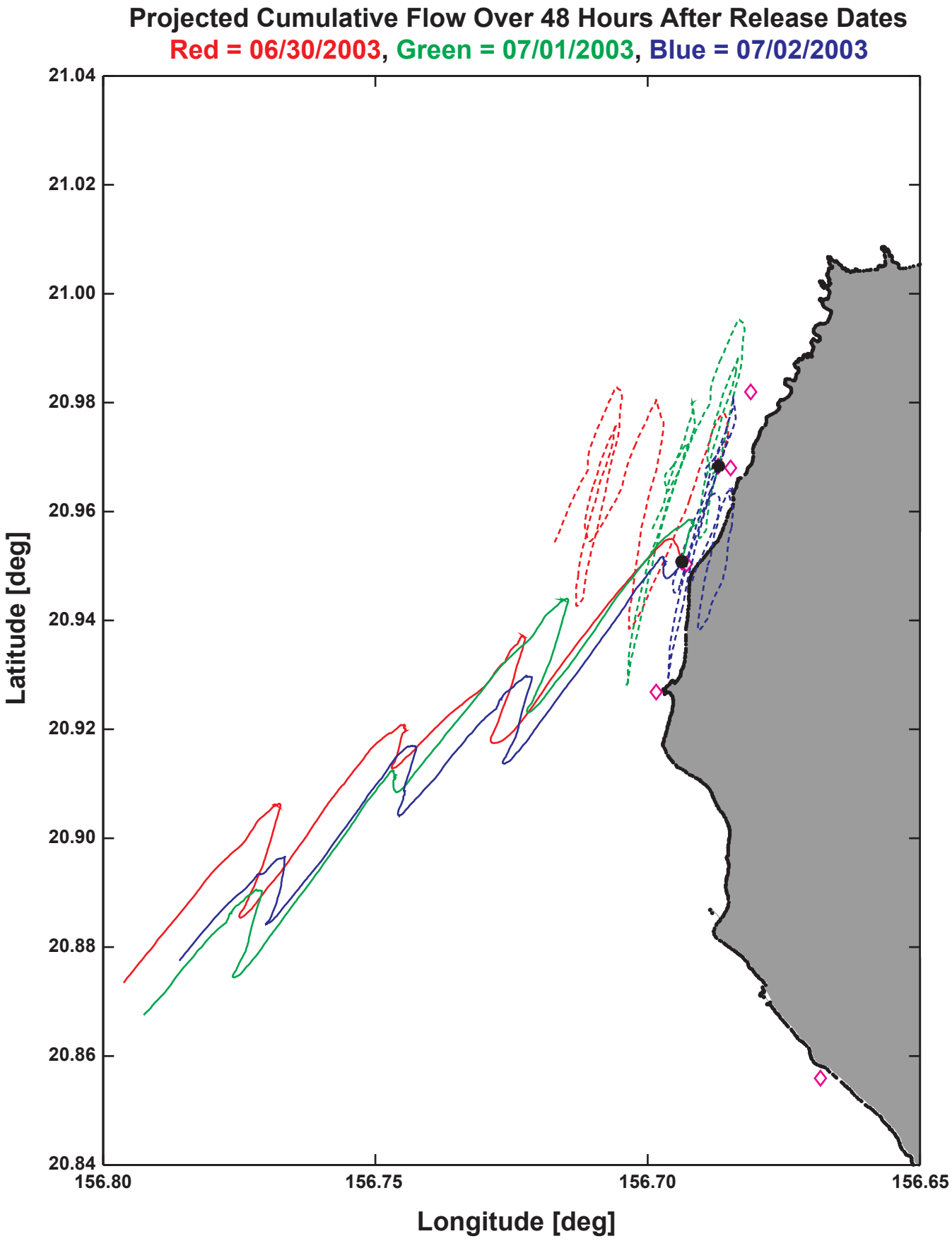

FIGURE 16. *48-hour progressive vector diagram of projected cumulative flow during the late June/early July Montipora capitata coral spawning. These data show projected near-surface particle trajectories over a 48-hour period starting at 21:00 hours on the specified dates. These calculations make the assumption that the flow measured at the instrument site is uniform alongshore, which is rarely the case.*

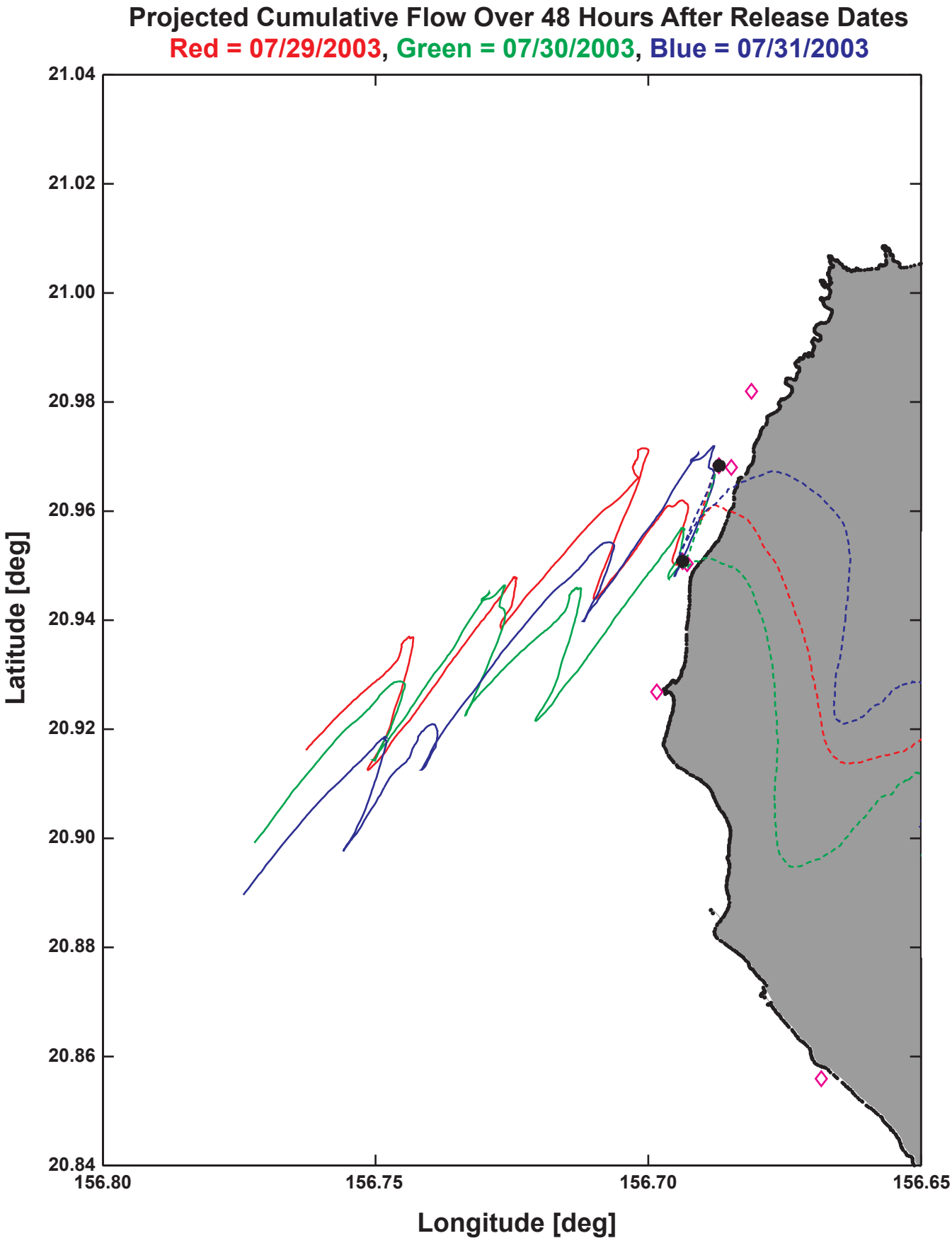

FIGURE 17. *48-hour progressive vector diagram of projected cumulative flow during the late July Montipora capitata coral spawning. These data show projected near-surface particle trajectories over a 48-hour period starting at 21:00 hours on the specified dates. These calculations make the assumption that the flow measured at the instrument site is uniform alongshore, which is rarely the case.*

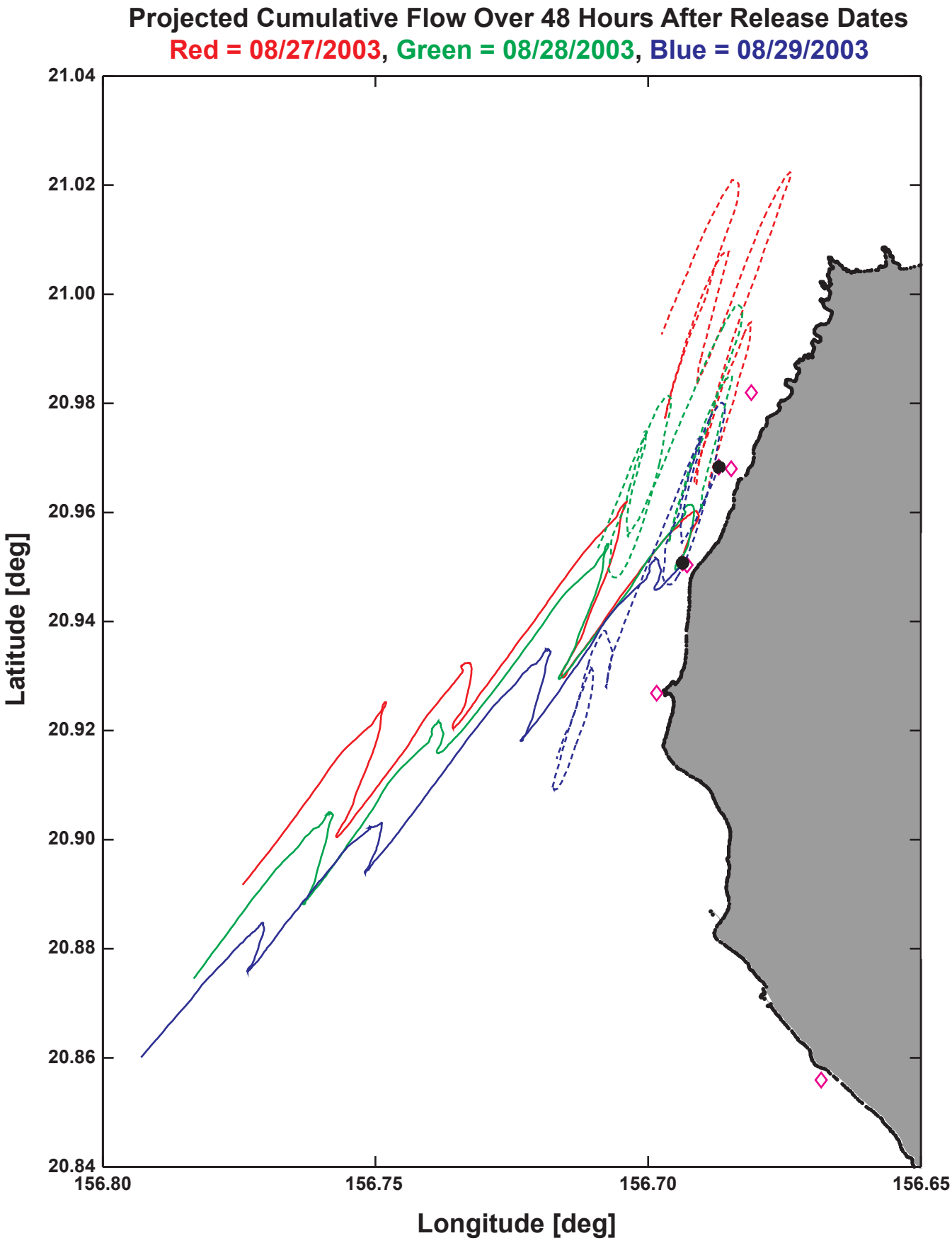

FIGURE 18. *48-hour progressive vector diagram of projected cumulative flow during the late August Montipora capitata coral spawning. These data show projected near-surface particle trajectories over a 48-hour period starting at 21:00 hours on the specified dates. These calculations make the assumption that the flow measured at the instrument site is uniform alongshore, which is rarely the case.*

retained nearby and could have possibly reached as far north as the headland at Napili and as far south as Kaanapali within 48 hours of release. The 48-hour progressive vector diagrams of projected cumulative flow from the Honokawai site are shown in for the same spawning events (solid lines). These data show that there was strong net alongshore flow to the south and slight offshore flow to the west off the Honokawai site, causing net projected larval transport to be to the south and offshore. Observations by Storlazzi and Jaffe (2003) and Storlazzi et al. (2003) demonstrate that current speeds are greater further offshore, suggesting that coral larvae released from these reefs were transported far away from the site.

CONCLUSIONS

In all, more than 29,300 observations of currents, waves and water column properties were collected per day for 108 days over the course of 3 months between July and October, 2003, off West Maui, Hawaii, USA. Critical findings from these measurements and analyses include:

(1) Tidal currents rise to the northeast and fall to the southwest off Honokawai and South Kahana.

(2) Flow along the 10 m isobath is primarily controlled by the tides at higher frequencies (<26 hours) and by winds or sea level variations at lower frequencies (> 36 hours). Off Southern Kahana the net flow during the experiment was to the north while off Honokawai the net flow was to the south, demonstrating that this area is a region of divergence in net flow.

(3) Waves are predominantly from the south during the summer months; the northern portion of the study area was not substantially impacted by wave-induced near-bed shear stresses during the experiment. Southern Ocean swell is typically confined to south of Black Rock Point at Kaanapali but sometimes can propagate all the way north to Northern Kahana.

(4) Temperature along the study area rose throughout the course of the experiment. Large daily fluctuations in temperature were observed and were correlated to different phases of the tides.

(5) Salinity varied substantially both temporally and spatially throughout the study area over the course of the experiment, often changing quite rapidly. Numerous low salinity departures were observed in the latter portion of the experiment, and the cause is unknown. Possible factors include stream discharge and local discharge of submarine groundwater.

(6) Higher turbidity is typically observed during large wave events, strong Trade winds, and falling tides.

(7) Modeled projected coral larvae trajectories show two dominant patterns based on the flow recorded at the two main study sites off South Kahana and Honokawai during the Julian Day 179-181 spawning. Coral larvae released off South Kahana were projected to be retained in the region between North Kahana and South Kahana, while those released off Honokawai were projected to be carried offshore to the south.

These data provide us with a much clearer picture of the nature of and controls on flow and suspended particulate flux in the study area. A number of interesting phenomena were observed that indicate the complex hydrography off West Maui. The observed flow patterns and hydrography presented here can be used by future studies to predict he dispersal of sediment, contaminants, nutrients and/or coral larvae and may provide insight into the varied nature of coral reef health and distribution along West Maui.

ACKNOWLEDGEMENTS

This work was carried out as part of the USGS's Coral Reef Project as part of an effort in the U.S. and its trust territories to better understand the affect of geologic processes on coral reef systems. Andrea Ogston and Kathy Presto contributed as part of the ongoing USGS/University of Washington's Cooperative Studies Program. We would like to thank Joe Reich, the captain of the *R/V Alyce C.*, who piloted and navigated during the coral coverage surveys and during our numerous instrument deployments. As always, Eric Brown (University of Hawaii's Institute for Marine Biology) overextended himself, helping us with everything from determining the experiment sites, to cleaning and checking the instrument package to just being a great guy with good advice. We would also like to thank Greg Piniak (USGS) and Amy Draut (USGS), who contributed numerous excellent suggestions and a timely review of our work.

LITERATURE CITED

Storlazzi, C.D. and Jaffe, B.E., 2003. "Coastal Circulation and Sediment Dynamics along West Maui, Hawaii, PART I: Long-term measurements of currents, temperature, salinity and turbidity off Kahana, West Maui: 2001-2003." *U.S. Geological Survey Open-File Report 03-482*, 28 p.

Storlazzi, C.D., Logan, J.B., McManus, M.A., and McLaughlin, B.E., 2003. "Coastal Circulation and Sediment Dynamics along West Maui, Hawaii, PART II: Hydrographic Survey Cruises A-3-03-HW and A-4-03-HW Report on the spatial structure of currents, temperature, salinity and turbidity along Western Maui." *U.S. Geological Survey Open-File Report 03-430*, 50 p.

TABLE 1. Experiment personnel

Person	Affiliation	Responsibilities
Curt Storlazzi	USGS	Chief scientist, led scuba diving operations
Michael Field	USGS	Project chief, scuba diver
Andrea Ogston	UW	Scientist
Joshua Logan	USGS	Oversaw navigation, co-led scuba diving operations
Katny Presto	UW	Instrument support
Dave Gonzales	USGS	Instrument support
Greg Piniak	USGS	Scuba diver, instrument support
Joe Reich		Captain, *R/V Alyce C.*

TABLE 2. Instrument package sensors

Instrument	Sensors
MiniPROBE-1	RD Instruments 600 kHz Workhorse Monitor acoustic doppler current profiler (upward-looking) NIWA Dobie-A strain gauge pressure sensor Aqautec/Seapoint 200-TY optical backscatter sensor
MiniPROBE-2	RD Instruments 600 kHz Workhorse Monitor acoustic doppler current profiler (upward-looking) NIWA Dobie-A strain gauge pressure sensor Aqautec/Seapoint 200-TY optical backscatter sensor
MegaDOBIE	NIWA Dobie-A strain gauge pressure sensor Aqautec/Seapoint 200-TY optical backscatter sensor Seabird SBE-37SM Microcat conductivity-temperature sensor
SuperDOBIE-1	NIWA Dobie-A strain gauge pressure sensor Seabird SBE-37SM Microcat conductivity-temperature sensor
SuperDOBIE-2	NIWA Dobie-A strain gauge pressure sensor Seabird SBE-37SM Microcat conductivity-temperature sensor
DOBIE	NIWA Dobie-A strain gauge pressure sensor
Weather Station	NovaLynx WS-16 Weather Station with anemometer, air temperature and precipitation sensors

TABLE 3. Instrument package deployment log: 06/2003 - 10/2003

Location	Instrument	Island ID	Depth [m]	Location	Latitude [dd]	Longitude [dd]
1	MegaDOBIE	MA	10	Honolua	21.01523	-156.63997
2	SuperDOBIE-1	MA	10	North Kahana	20.98198	-156.68108
3	MiniPROBE-2	MA	10	South Kahana	20.96833	-156.68704
4	MiniPROBE-1	MA	10	Honokawai	20.95078	-156.69365
5	DOBIE	MA	10	Kaanapali	20.92684	-156.69845
6	SuperDOBIE-2	MA	10	Puumana	20.85593	-156.66826
7	Weather Station	MA	-	Honokawai	20.94893	-156.69107

TABLE 4. Wave statistics during the experiment

Location	Hsig [m]	Tdom [sec]	taub [N/m^2]
Honolua	0.04 ± 0.03	5.61 ± 1.39	0.012 ± 0.010
North Kahana	0.16 ± 0.07	5.92 ± 2.71	0.163 ± 0.077
South Kahana	0.16 ± 0.05	8.02 ± 1.18	0.074 ± 0.039
Honokawai	0.13 ± 0.04	8.01 ± 1.30	0.052 ± 0.023
Kaanapali	0.21 ± 0.08	9.07 ± 1.44	0.104 ± 0.060
Puumana	0.31 ± 0.11	9.70 ± 1.97	0.220 ± 0.123

The statistics shown are the mean ± 1 standard deviation

TABLE 5. Temperature and salinity statistics during the experiment

Location	Temp [°C]	Salinity [PSU]
Honolua	26.13 ± 0.51	34.857 ± 0.140
North Kahana	26.31 ± 0.57	34.724 ± 0.254
South Kahana	26.54 ± 0.54	No data
Honokawai	26.57 ± 0.56	No data
Puumana	26.74 ± 0.52	34.486 ± 0.256

The statistics shown are the mean ± 1 standard deviation

APPENDIX 1

Acoustic Doppler Current Profiler (ADCP) Information

Instrument:

RD Instruments 600 kHz Workhorse Monitor

Transmitting Frequency:	614 kHz
Depth of Transducer:	10 m
Blanking Distance:	0.25 m
Height of First Bin above Bed:	0.75 m
Bin Size:	1.0 m
Number of Bins:	12
Operating Mode:	High-resolution, broad bandwidth
Sampling Frequency:	4 Hz
Beam Angle:	20 deg
Time per Ping:	00:00:00.30
Pings per Ensemble:	1
Ensemble Interval:	00:04:00.00
Sound Speed Calculation:	Set salinity, updating temperature via sensor

Data Processing:

The data were averaged over 20-bin (1 hour) ensembles, all of the spurious data above the water surface were removed and all of the data in bins where the beam correlation dropped below 70% were removed for visualization and analysis.

Position Information:

Garmin GPS-76 GPS

RDI internal compass/gyroscope, set to –10 deg magnetic offset

APPENDIX 2

External Sensor Information

Instruments:

NIWA Dobie-A Pressure Sensor

Depth of Transducer:	10 m
Operating Mode:	Water level time series
Sampling Frequency:	2 Hz
Measurements per Burst:	1024
Time Between Bursts:	01:00:00.00

Aqautec/Seapoint 200-TY self-logging Optical Backscatter Sensor (SLOBS)

Sampling Frequency:	2 Hz
Measurements per Burst:	30
Time Between Bursts:	00:04:00.00

Seabird Microcat SBE-39SM Conductivity and Temperature Sensor (CT)

Sampling Frequency:	2 Hz
Measurements per Burst:	30
Time Between Bursts:	00:04:00.00

NovaLynx WS-16 Weather Station

Sampling Frequency:	1 Hz
Measurements per Burst:	30
Time Between Bursts:	00:30:00.00

Data Processing:

The Dobie water level data were averaged over the entire 20 min burst to compute tidal height while hourly significant wave height and dominant wave period data were computed spectrally using the USACE SUPERDUCK method. The SLOBS and CT data were post-processed for visualization and analysis by removing all instantaneous (only one data point in time) data spikes that exceeded the deployment mean + 3 standard deviations.

Position Information:

Garmin GPS-76 GPS